K. Ganesh Kadiyala, Vanipenta Yamini, Kommuru Goutham
and Naresh Kumar Katari*

3 Rare earth metal-catalyzed multicomponent reactions

3.1 Introduction

Multicomponent reactions (MCRs) are one-pot synthetic processes that involve at least three commercially available or easily accessible substrates that combine together to produce a single product through cascade reactions [1]. MCRs are advantageous and popular because of their atom-economy and step-efficiency, which reduce waste generation. In particular, their ease of use and their adaptability to experimental techniques reveal their entries to a broad array of synthetic compounds over the multiple combination opportunities of coupling reagents. The Strecker reaction was the first ever reported example of such an MCR reaction in which α-aminonitriles were synthesized from aldehydes. Following Strecker's synthesis, the chemical community rapidly progressed to further carbonyl-based MCRs. The well-known aldehyde-based MCR is the Mannich reaction, which yields an iminium intermediate, which is obtained from formaldehyde and amines, either primary or secondary, which reacts with carbonyl compound to afford β-aminocarbonyls [2]; and the Biginelli reaction converts an aldehyde, a β-ketoester, and urea into dihydropyrimidones [3]. Simultaneously, isocyanide-based MCRs are also developed. The first isocyanide-based MCRs report, Passerini reaction [4], was published in 1921 and rapidly attained prominence in the pharmaceutical sector. The Ugi condensation [5], another foremost isocyanide-based MCR that consists of an aldehyde, an amine, a carboxylic acid, and an isocyanide, allows for the hasty assembly of libraries of α-aminoacyl amide derivatives, making it useful for drug development.

Nowadays, the overall demand for practical and effective synthetic methods propels new research and encourages the creative rethinking of well-established ideas. The desire for sustainable energy and atom-efficient reactions are driving an increase in the demand for Lewis acid-catalyzed multicomponent reaction methods, which open up new avenues in synthetic organic chemistry. Rare earth metal-induced MCRs

*Corresponding author: Naresh Kumar Katari, Department of Chemistry, School of Science, GITAM Deemed to be University, Hyderabad, India, e-mail: nkatari@gitam.edu
K. Ganesh Kadiyala, Depatment of Chemistry, Shri Vishnu Engineering College for Women, Bhimavaram, Andhra Pradesh, India
Vanipenta Yamini, Sri A. S. N. M. Govt. College (A), Palakollu, Andhra Pradesh, India
Kommuru Gowtham, Indian Institute of Chemical Technology, Hyderabad, Telangana, India

https://doi.org/10.1515/9783110788082-003

are one of the Lewis acid catalysts that are currently developing, although significant advancements are anticipated in this area shortly.

3.2 Various organic synthesis using rare earth metals as catalysts

3.2.1 Synthesis of substituted pyrroles derivatives

Pyrrole is an important constituent of porphyrin, chlorophyll, and bile pigment. It is also a main scaffold of amino acids such as proline and hydroxyproline. In addition to these prevalent compounds, pyrrole structural fragments are particularly found in natural products of marine origin. The most prominent and well-known method for the preparation of pyrrole is Paal-Knorr synthesis [6, 7]. Depending on the importance of pyrrole moiety, several scientific communities have showcased various synthetic protocols [8, 9] for the preparation of pyrrole scaffold.

Shiraishi and co-workers [10] developed an efficient and mild MCR protocol for the synthesis of multi-substituted pyrrole compounds (**4**) (Figure 3.1). The protocol involves the reaction of rare earth metal SmI_2 or $SmCl_3$-catalyzed coupling of amines (**1**), aldehydes (**2**), and nitroalkane (**3**).

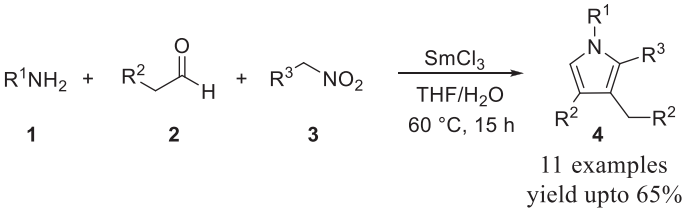

Figure 3.1: Synthesis of samarium catalyzed pyrroles through MCR.

This MCR sequence involves the reaction of amine (**1**) and aldehyde (**2**) to form imine (**A**), which undergoes aldol condensation with aldehyde (**2**) in the presence of samarium catalyst to give α, β-unsaturated imine (**B**). The obtained α, β-unsaturated imine (**B**) reacts with nitroalkane (**3**) under heating, following the Michael addition adduct (**C**), proton abstraction adduct (**D**), cyclization, and isomerization (**E**), giving multi-substituted pyrrole derivatives (**4**) (Figure 3.2). The present protocol is suitable for aldimines, but is a limitation for ketimines obtained from the condensation of ketones and amines.

Encouraged by the synthesis of samarium (III)-catalyzed pyrroles, the same group developed a diversified protocol for the regioselective construction of pyrroles (**7**) by the reaction of nitroalkenes (**6**) and imines (**8**) under samarium catalysis (Figure 3.3) [11]. In this protocol, a wide range of nitro alkenes (**6**) (obtained from amines (**1**) and

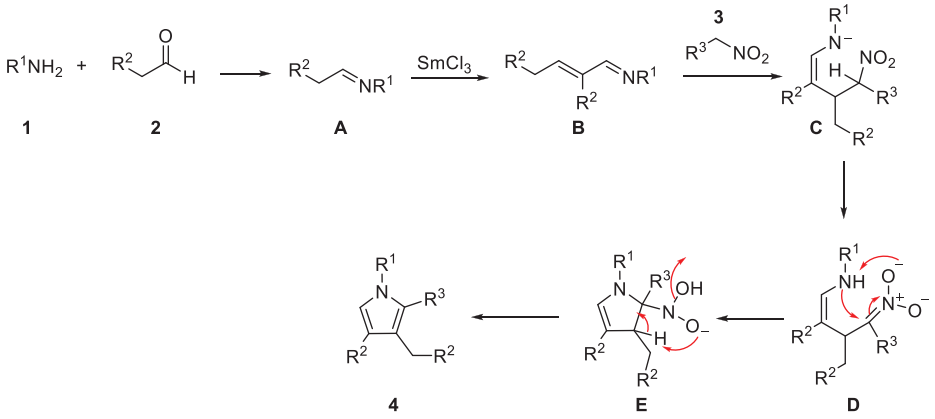

Figure 3.2: Reaction mechanism of samarium (III)-catalyzed pyrroles synthesis through MCR.

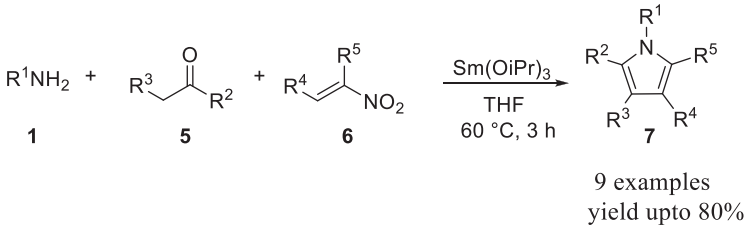

Figure 3.3: Synthesis of pyrroles via samarium-catalyzed MCRs.

an aldehyde or ketones (**5**)) (Figure 3.4) and imines (**8**) were combined to generate substituted pyrroles (7) as well as fused pyrrole derivatives in moderate to good yields. The yield of the pyrrole derivative was affected by the substituent alkyl group attached to the nitrogen atom of imines. As the bulkiness of the alkyl group increases, yield of the corresponding pyrrole derivative decreases.

3.2.2 Synthesis of functionalized dihydropyrimidine derivatives via Biginelli condensation

Dihydropyrimidines (DHPMs) are a class of nitrogen-containing complexes heterocyclic scaffolds that are present in several marine alkaloids (such as crambine and batzelladine) [12]. In addition, it has been found that they are effective HIV gp-120CD4 inhibitors [13]. Besides, a number of multi-functionalized dihydropyrimidines also reveal antitumor [14], antibacterial [15], antiviral [16], and anti-inflammatory properties [17] in addition to having exceptional pharmacological effectiveness. Despite many

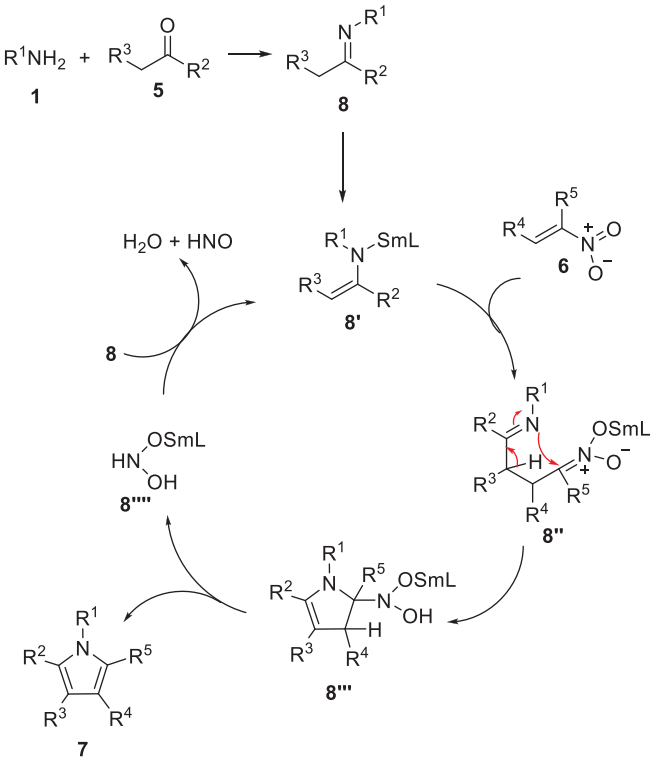

Figure 3.4: Reaction mechanism of samarium (III)-catalyzed pyrroles synthesis through MCR.

approaches that have materialized [18–26], still it requires mild protocols for the construction of dihydropyrimidine derivatives.

Ma and co-workers [27] reported an highly efficient $Yb(OTf)_3$-mediated multicomponent reaction of aldehydes (**9**), urea (**10**), and β-ketoesters (**11**), via the Biginelli reaction for the preparation of dihydropyrimidines (**12**) under a solvent-free environment at 100 °C (Figure 3.5). Replacing β-ketoesters with 1,3-diketones, the reaction proceeds smoothly, furnishing dihydropyrimidines.

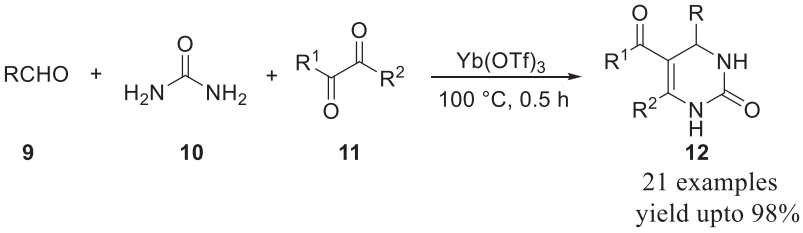

Figure 3.5: Synthesis of dihydropyrimidines via $Yb(OTf)_3$-catalyzed MCRs.

A representative procedure for the synthesis of pyrimidinones (**15**) was provided by Narasaiah et al. [28] via multicomponent reaction of urea (**10**), *β*-ketoesters(**13**), and aldehydes (**14**) under samarium catalysis (Figure 3.6). The present protocol involves the elimination of tedious work-up process for the purification of products. Purification of products encompasses the removal of the solvent under reduced pressure. The resulting residue was mixed with crushed ice for a while, filtered, dried, and purified by recrystallization from methanol.

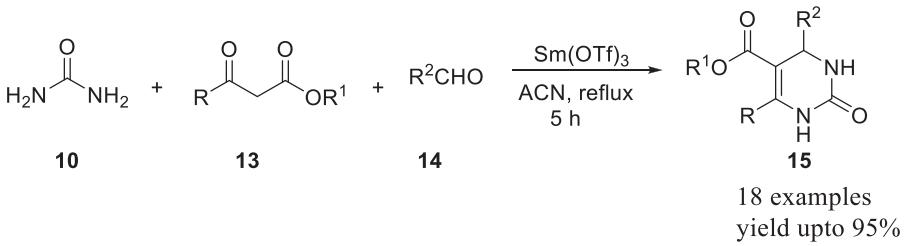

Figure 3.6: Synthesis of dihydropyrimidines via $Sm(OTf)_3$-catalyzed MCRs.

Complex optically active dihydropyrimidines (**17**) have been generated utilizing a highly enantioselective multicomponent reactions using Biginelli condensation, and employing a recyclable asymmetric $Yb(OTf)_3$ catalyst with a new hexadentate chiral ligand (**L**) (Figure 3.7) [29]. The reaction produces high yields of dihydropyrimidines with decent enantioselectivity (Figure 3.7–I). A suggested transition state model assigned the product's absolute configuration. The acylimine intermediate produced in situ might coordinate with the Yb atom. The pyridyl group shielded the coordinated acylimine's *si*-face, allowing the enol ester to attack as nucleophile from the re-face.

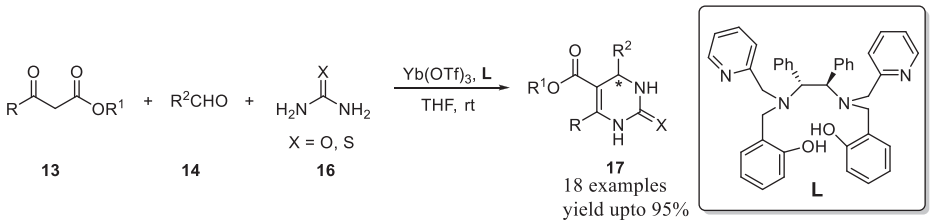

Figure 3.7: Asymmetric synthesis of dihydropyrimidines via $Yb(OTf)_3$-catalyzed MCRs.

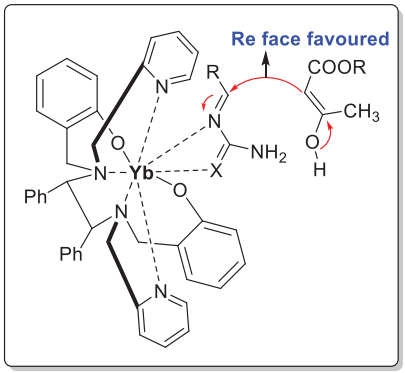

Figure 3.7-I: Transition state model showing *Re*-face attack of enol.

3.2.3 Synthesis of nitrogen containing compounds via Ugi reaction

Ugi reaction constitutes 4-component coupling (4CC) of amines, aldehydes, carboxylic acid, and isonitriles for the construction of libraries of nitrogen-containing compounds [30]. Keung and co-workers [31] have demonstrated scadium triflate-catalyzed variable Ugi three component coupling reaction for the synthesis of *α*-aminoamidine derivatives (Figure 3.8). This new method revealed a novel route for the preparation of imidopyrazine (**24**) (Figure 3.9) and hydantoin imide (**27**) (Figure 3.10).

Okandeji et al. [32] reported a high yielding multicomponent Ugi reaction using sub-stoichiometric amounts of ytterbium and scandium triflate catalysts for the production of α-acylamino carboxamide (**30** and **31**) (Figure 3.11). The activation of the imine intermediate of this multicomponent reaction is principally responsible for the

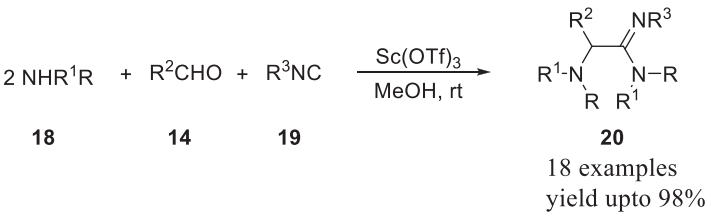

Figure 3.8: $Sc(OTf)_3$-mediated variable MCRs for constructing *α*-aminoamidine.

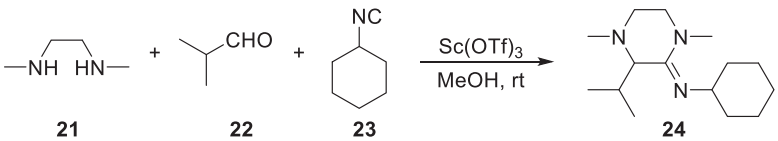

Figure 3.9: $Sc(OTf)_3$-mediated variable MCRs for assembling imidopyrazine.

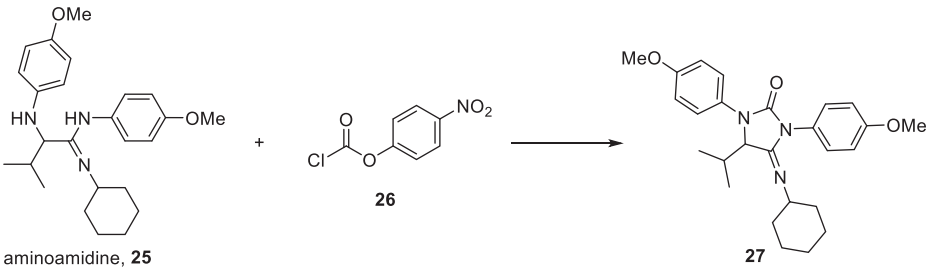

Figure 3.10: $Sc(OTf)_3$-mediatedhydantoin imide preparation via MCRs.

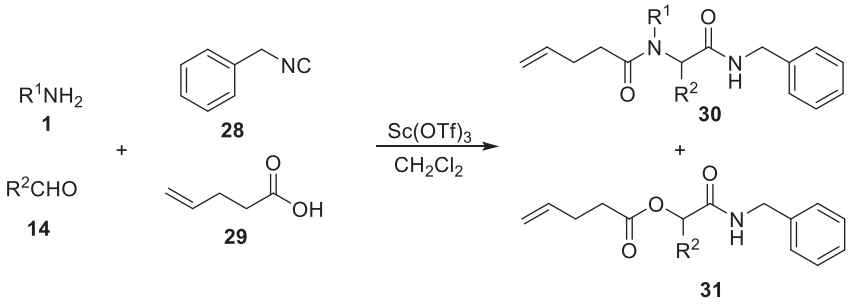

Figure 3.11: $Sc(OTf)_3$-catalyzed Ugi4CC for the synthesis of α-acylamino carboxamide.

improvement in product yield. The possibility of realizing catalytic asymmetric Ugi 4CC reactions is encouraged by the apparent mechanism of catalysis, the striking variations in yield between the catalyzed and uncatalyzed reactions, and the accessibility of chiral Sc(III) complexes.

3.2.4 Synthesis of oxazolidinones

In 2016, Xu et al. [33] reported a three component coupling of propylene oxide (PO) (**32**), carbon dioxide (**33**), and substituted anilines (**34**) for the synthesis of oxazolidinones (**35**) under rare earth metal catalyst stabilized by amine-bridged tri-(phenolato) ligands (**L1-L6**) (Figure 3.12). In this reaction, a series of rare earth metal catalyst stabilized by amine-bridged tri-(phenolato) ligands complexes were prepared and studied for their catalytic efficiency (Figure 3.13). Complexes with electron-withdrawing group attached to the aromatic ring increase the acidity of the rare earth metal, which in turn enhances the activity of substrates, leading to quantitative yields of oxazolidinones (**35**). Excess ratio of PO (**32**)-to-aniline (**34**) was essential for the significant increase in the yield of the product. Ortho-substituted, irrespective of electron-donation or withdrawing anilines, and aliphatic amines were unsuitable for this conversion.

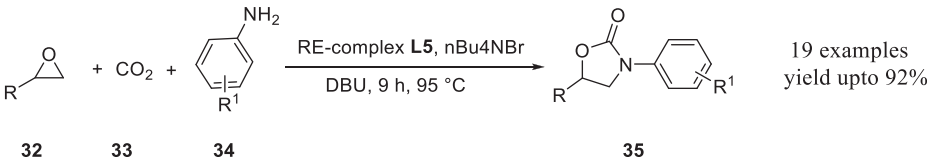

Figure 3.12: Nd-complex-catalyzed 3CC for the synthesis of oxazalidinones.

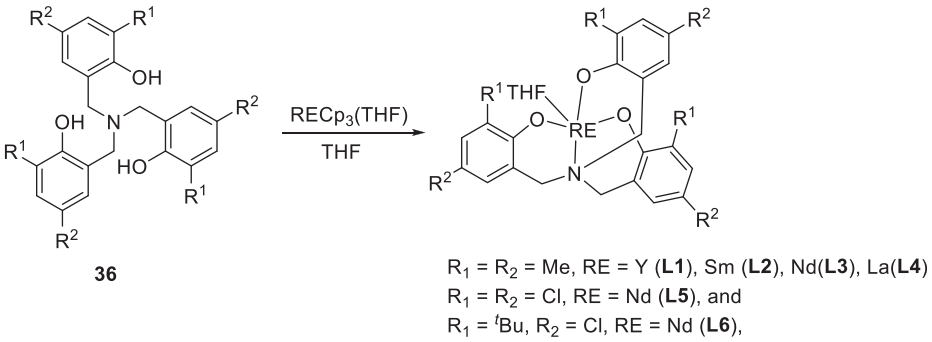

Figure 3.13: Synthesis of rare earth metal catalyst stabilized by amine-bridged tri-(phenolato) ligand complexes.

Pioneering work on 3 CC reactions for the synthesis of oxazolidinones provided the first report of 3-aryloxazolidinone (**35**) synthesis from easily available three component coupling of epoxide (**32**), aniline (**34**), and dialkyl carbonate (**37**) (ratio 2:1:2), under solvent-free rare earth metal amide catalysis (Figure 3.14) [34]. In addition, the reaction produces MeOH as the byproduct. The reaction is limited to monosubstituted epoxides, whereas in the reaction with vicinal disubstituted epoxides, the reaction is sluggish or does not takes place. Catalytic efficiency of metal amides decreases with decrease in ionic radii of rare earth metal ions.

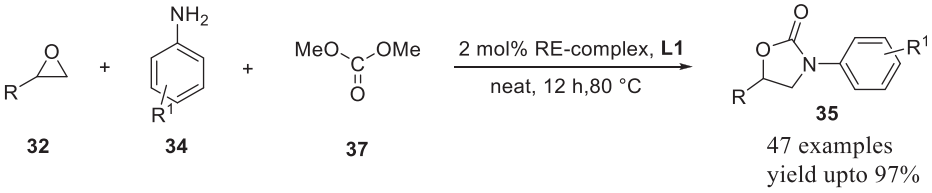

Figure 3.14: Synthesis of oxazolidinones, catalyzed by rare earth metal amide.

Cerric ammonium nitrate (CAN)-mediated synthesis of Betti bases (**40**) [35] from commercially available substrates *viz*. aryl and alkylamines (**34**), substituted benzaldehydes (**38**), and 2-naphthol (**39**), (1:1.2:1) was reported by Mekheimer et al. [36] (Figure 3.15).

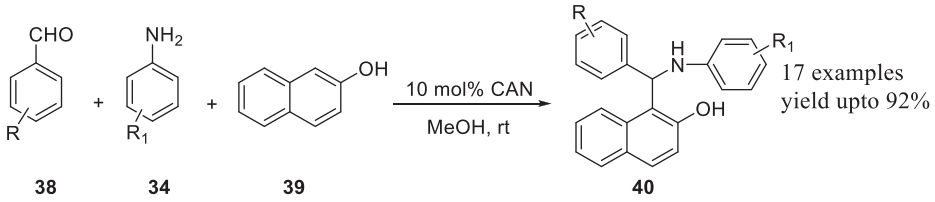

Figure 3.15: CAN-mediated synthesis of Betti base.

The reaction works well in ambient conditions with moderate-to-good yields in methanol. When the methanol was replaced by water, the reaction furnishes Schiff base, instead of betti base.

3.2.5 Synthesis of 3-aminoimidazoles

Rapid and efficient microwave-assisted 3 component coupling (3 CC) Ugi reaction of amidine (**41**), isocyanides (**19**), and aldehydes (**14**) for the synthesis of libraries of 3-aminoimidazoles (**42**), catalyzed by scandium triflate in methanol was described by Ireland and co-workers [37] (Figure 3.16). A variety of combinations of amidine (**41**), aldehydes (**14**), and isocyanides (**19**) undergo coupling to give a wide range of aminoimidazoles (**42**). The reaction was completed in a very short span of 10 min.

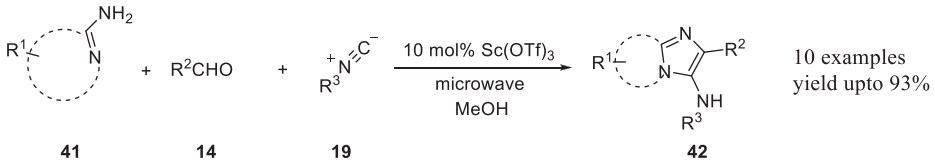

Figure 3.16: Microwave-assisted $Sc(OTf)_3$-catalyzed 3 CC Ugi reaction for the formation of 3-aminoimidazoles.

Hulme et al. [38] proposed a related 3 component coupling reaction for the synthesis of 3-aminoimidazopyridines (**45**) under microwave irradiation, catalyzed by scandium triflate using simply accessible reactants – 2-aminopyridine (**43**), trimethylsilylcyanide (**44**), (TMSCN, anisonitrile equivalent), and aldehyde (**14**) in methanol (Figure 3.17).

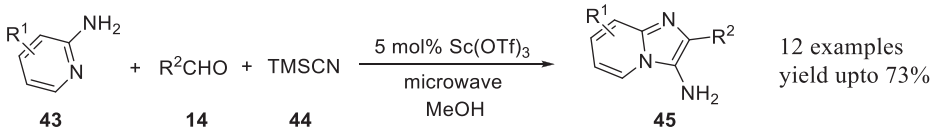

Figure 3.17: $Sc(OTf)_3$-catalyzed formation of 3-aminoimidazopyridines under microwave conditions.

3.2.6 Synthesis of quinoline derivatives via Pavarov reaction

In 2011, Vicente-García et al. [39] reported an effective $Sc(OTf)_3$-mediated domino Pavarov reaction [40] for the synthesis of diverse heterocycle tetrahydro-quinoline derivatives (**47**) by employing oxa-, thia-, and imidazolones as a novel class of electron-rich olefin partner (**46**) (dienophile) interaction with anilines (**34**) and aldehydes (**14**) (Figure 3.18). The use of a new class of olefin (dienophile) opens up a new direction for the construction of structural diversity of tetrahydroquinoline derivatives. The obtained MCR adducts were conveniently oxidized to yield the corresponding quinolones (**48**).

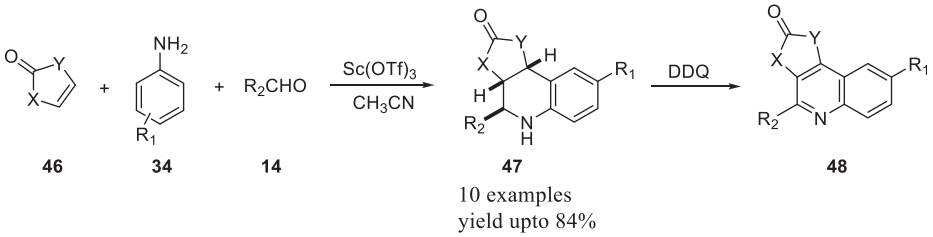

Figure 3.18: $Sc(OTf)_3$-catalyzed multicomponent Pavarov reaction toward the construction of quinolone derivatives.

Dhanapal et al. [41] reported scandium(III) triflate-catalyzed Povarov reaction between *para*-substituted anilines (**34**), vinyl pyrrolidone (**49**), and phenanthrene-9-carbaldehyde (**50**) for the synthesis of quinolines (**51**) as fluorescence probes for bacteria detection (Figure 3.19). The reaction was conducted at room temperature using $Sc(OTf)_3$ in acetonitrile to produce *cis*-2-(phenanthren-10-yl)-4-(2-oxopyrrolin-1-yl)tetrahydroquinoline intermediates that could then be further oxidized with DDQ in refluxing methylbenzene (toluene) to produce the corresponding quinoline derivatives (**51**).

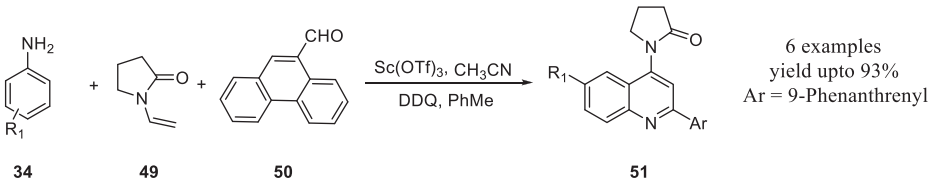

Figure 3.19: Pavarov multicomponent assembly of quinolone catalyzed by $Sc(OTf)_3$.

3.3 Conclusions

In conclusion, we have showcased the synthetic utility of rare earth metal complexes toward the synthesis of carbon and nitrogen heterocyclic compounds. Albeit, rare earth metal complexes are expensive compared to standard transition metal complexes, they are frequently employed in sub-sub-stoichiometric amounts. It is significant to note that the rare earth metal complexes are active in aqueous environment, eliminating the need for laborious drying process of the reaction conditions. Despite great contributions made in multicomponent reaction by using rare earth metal complexes, there is still room for further development and applications of water-tolerant rare earth complexes in sustainable MCR methodologies. It is also important to encourage the research community to develop advanced methods for the recovery and recycling of rare earth metal complexes. Additionally, investigation on the sequential MCRs with rare earth complexes would permit chemists to construct heterocyclic scaffolds with great complexity and biological profiles.

References

[1] Strecker, A. On the artificial formation of lactic acid and a new body homologous to glycocoll.Ann Chem Pharm, 1850, 75, 27–45.
[2] Blicke, FF. The Mannich reaction. Org React, 1942, 1, 303–341.
[3] Biginelli, P, Gazz, P. Synthesis of 3,4-Dihydropyrimidin-2(1*H*)-ones. Chim Ital, 1893, 23, 360–416.
[4] Passerini, M, Simone, L. Composto del *p*-isonitril-azobenzoloconacetone ed acidoacetico. Gazz Chim Ital, 1921, 51, 126–129.
[5] Ugi, I, Meyr, R, Fetzer, U, Steinbrückner, C. VersuchemitIsonitrilen. Angew Chem, 1959, 71, 386–386.
[6] Paal, C. Ueber die derivate des acetophenonacetessigesters und des acetonylacetessigesters. Berichte der deutschenchemischen Gesellschaft, 1884, vol 17, 2756–2767.
[7] Knorr, L. Synthese von furfuran derivatenaus dem diacetbernsteinsäureester. Berichtederdeutschenchemischen Gesellschaft, 1884, 17, 2863–2870.
[8] Tzankova, D, Vladimirova, S, Peikova, L, Georgieva, MJ. Synthesis of pyrrole and substituted pyrroles. Chem Technol Metall, 2018, 53, 451–464.
[9] Estévez, V, Villacampa, M, Menéndez, JC. Recent advances in the synthesis of pyrroles by multicomponent reactions. Chem Soc Rev, 2014, 43, 4633–4657.
[10] Shiraishi, H, Nishitani, T, Sakaguchi, S, Ishii, Y. Preparation of substituted alkyl pyrroles via samarium-catalyzed three-component coupling reaction of aldehydes, amines, and nitroalkanes. J Org Chem, 1998, 63, 6234–6238.
[11] Shiraishi, H, Nishitani, T, Nishihara, T, Sakaguchi, S, Ishii, Y. Regioselective synthesis of alkylpyrroles from imines and nitroalkenes by lanthanide compounds. Tetrahedron, 1999, 55, 13957–13964.
[12] Hegedüs, A, Hell, Z, Vígh, I. Convenient one-pot heterogeneous catalytic method for the preparation of 3,4-Dihydropyrimidin-2(1*H*)-ones. Synth Commun, 2006, 36, 129–136.
[13] Patil, AD, Kumar, NV, Kokke, WC, Bean, MF, Freyer, AF, De Brosse, C, Mai, S, Truneh, A, Faulkner, DJ, Carte, B, Breen, AL, Hertzberg, RP, Johnson, RK, Westley, JW, Potts, BCM. Novel alkaloids from the spongeBatzella sp.: Inhibitors of HIV gp120-Human CD4 binding. J Org Chem, 1995, 60, 1182–1188.

[14] Peters, T, Lindenmaier, H, Haefeli, W, Weiss, J. Interaction of the mitotic kinesin Eg5 inhibitor monastrol with P-glycoprotein. Naunyn Schmiedebergs Arch Pharmacol, 2006, 372, 291–299.
[15] Choi, SH, McCollum, D. A role for metaphase spindle elongation forces in correction of merotelic kinetochore attachments. Curr Biol, 2012, 22, 225–230.
[16] Cochran, JC, Gilbert, SP. ATPase mechanism of Eg5 in the absence of microtubules: Insight into microtubule activation and allosteric inhibition by monastrol. Bio chem, 2005, 44, 16633–16648.
[17] Tcherniuk, S, van Lis, R, Kozielski, F, Skoufias, DA. Mutations in the human kinesin Eg5 that confer resistance to monastrol and S-trityl-l-cysteine in tumor derived cell lines. Bio chem Pharmacol, 2010, 79, 864–872.
[18] Kappe, CO. Recent advances in the Biginelli dihydropyrimidine synthesis new tricks from an old dog. Acc Chem Res, 2000, 33, 879–888.
[19] Armstrong, RW, Combs, AP, Tempest, PA, Brown, SD, Keating, TA. Multiple-component condensation strategies for combinatorial library synthesis. Acc ChemRes, 1996, 29, 123–131.
[20] Ramarao, AV, Gurjar, MK, Vasudevan, J. An enantiospecific synthesis of the tricyclic guanidine segment of the anti-HIV marine alkaloid batzelladine A. ChemCommun, 1995, 1369–1370.
[21] Atwal, KS, Swanson, BN, Unger, SE, Floyd, DM, Merelandm, S, Hedberg, A, O'Reilly, BC. Dihydropyrimidine calcium channel blockers. 3. 3-Carbamoyl-4-aryl-1,2,3,4-tetrahydro-6-methyl-5-pyrimidinecarboxylic acid esters as orally effective antihypertensive agents. J Med Chem, 1991, 34, 806–811.
[22] Aron, ZD, Overman, LE. The tethered Biginelli condensation in natural product synthesis. Chem Commun, 2004, 253–265.
[23] Kaur, R, Chaudhary, S, Kumar, K, Gupta, MK, Rawal, RK. Recent synthetic and medicinal perspectives of dihydropyrimidinones: A review. Eur J Med Chem, 2017, 132, 108–134.
[24] Hu, EH, Sidler, DR, Dolling, UH. Unprecedented catalytic three component one-pot condensation reaction: An efficient synthesis of 5-Alkoxycarbonyl-4-aryl-3,4-dihydropyrimidin-2(1*H*)-ones. J Org Chem, 1998, 63, 3454–3457.
[25] Yadav, JS, Reddy, BVS, Reddy, KB, Raj, KS, Prasad, AR. Ultrasound-accelerated synthesis of 3,4-dihydropyrimidin-2(1*H*)-ones with ceric ammonium nitrate. Perkin Trans, 2001, 1, 1939–1941.
[26] Sun, Q, Wang, Y, Ge, Z, Cheng, T, Li, R. A highly efficient solvent-free synthesis of dihydropyrimidinones catalyzed by zinc chloride. Synthesis, 2004, 7, 1047–1051.
[27] Ma, Y, Qian, C, Wang, L, Yang, M. Lanthanide triflate catalyzed Biginelli reaction. One-pot synthesis of dihydropyrimidinones under solvent-free conditions. J Org Chem, 2000, 65, 3864–3868.
[28] Narsaiah, AV, Reddy, AR, Yadav, JS. Samarium triflate-catalyzed Biginelli condensation: An improved method for the synthesis of 3,4-Dihydropyrimidin-2(1*H*)-ones. SynthCommun, 2011, 41, 2794–2799.
[29] Huang, Y, Yang, F, Zhu, C. Highly enantioseletive Biginelli reaction using a new chiral ytterbium catalyst: asymmetric synthesis of dihydropyrimidines. J Am Chem Soc, 2005, 127, 16386–16387.
[30] Ugi, I, Werner, B, Dömling, A. The chemistry of isocyanides, their multi component reactions and their libraries. Molecules, 2003, 8, 53–66.
[31] Keung, W, Bakir, F, Patron, AP, Rogers, D, Priest, CD, Darmohusodo, V. Novel α-amino amidine synthesis via scandium(III) triflate mediated 3CC Ugi condensation reaction. Tetrahedron Lett, 2004, 45, 733–737.
[32] Okandeji, BO, Gordon, JR, Sello, JK. Catalysis of Ugi four component coupling reactions by rare earth metal triflates. J Org Chem, 2008, 73, 5595–5597.
[33] Xu, B, Wang, P, Lv, M, Yuan, D, Yao, Y. Transformation of carbon dioxide into oxazolidinones and cyclic carbonates catalyzed by rare-earth-metal phenolates. Chem Cat Chem, 2016, 8, 2466–2471.
[34] Zhou, M, Zheng, X, Wang, Y, Yuan, D, Ya, Y. A multicomponent approach to oxazolidinone synthesis catalyzed by rare-earth metal amides. Chem Cat Chem, 2019, 11, 5783–5787.
[35] Cardellicchio, C, Capozzi, MAM, Naso, F. The Betti base: The awakening of a sleeping beauty. Tetrahedron Asymm, 2010, 21, 507–517.

[36] Mekheimer, RA, Asiri, AM, Abdel Hameed, AM, Awed, RR, Sadek, KU. An efficient multicomponent, one-pot synthesis of Betti bases catalyzed by cerium (IV) ammonium nitrate (CAN) at ambient temperature. Green Process Synth, 2016, 5, 365–369.
[37] Ireland, SM, Tye, H, Whittaker, M. Microwave-assisted multi-component synthesis of fused 3-aminoimidazoles. Tetrahedron Lett, 2003, 44, 4369–4371.
[38] Schwerkoske, J, Masquelin, T, Perunb, T, Hulme, C. New multi-component reaction accessing 3-aminoimidazo[1,2-a]pyridines. Tetrahedron Lett, 2005, 46, 8355–8357.
[39] Vicente-García, E, Ramón, R, Lavilla, R. New heterocyclic inputs for the Povarov multicomponent reaction. Synthesis (Stuttg), 2011, 2237–2246.
[40] Forero, JSB, Junior, JJ, da Silva, FM. The Povarov reaction as a versatile strategy for the preparation of 1,2,3,4-tetrahydroquinoline derivatives: An overview. Curr Org Synth, 2014, 12, 102–107.
[41] Dhanapal, R, Perumal, PT, Damodiran, M, Ramprasath, C, Mathivanan, N. Synthesis of quinoline derivatives for fluorescent imaging certain bacteria. Bioorg Med Chem Lett, 2012, 22, 6494–6497.

K Ganesh Kadiyala, Vanipenta Yamini, Kommuru Goutham
and Naresh Kumar Katari*

12 Photocatalysis of rare earth complexes in organic synthesis

12.1 Introduction

A traditional photochemical reaction to excite the substrate or reagents uses high-energy UV light. These reactions are often unselective, highly difficult to control and involve special equipment to carry out the reaction. Visible light has emerged as an effective reagent in photocatalysis, an effective technique in organic synthesis that utilizes photons for excitation, paving the path for sustainable chemical reactions. In this field new reactions were developed that are mostly focused on a common photo redox cycle. In addition, recently a variety of new concepts and strategies have also emerged that involve the application of visible light with variable wavelengths and intensities that tune the properties of photocatalyst to control the reactivity of the organic compounds. Evidenced by volumes of reviews published in the last decade, many research groups have turned their interest in photocatalysis [1–8]. In general, iridium- and ruthenium-based photocatalysis dominates the chemical community till now, but recently rare earth metal complexes [9, 10] are also employed as photocatalysts for various organic transformations.

12.2 General mechanistic pathways involved in photocatalysis

Photocatalysts could initiate the organic transformations through various mechanistic manners. Particularly, visible light photoredox catalysis [11–15] is documented as an effective protocol in synthetic organic conversions. The various mechanistic cycles of photocatalysis are shown in Figure 12.1. Depending on the reagents and substrates present in the reaction mixture, an excited photocatalyst (PC*) may absorb or donate a single electron after being exposed to light, enabling oxidative or reductive quenching cycles. Occasionally, a coordinated proton transfer (proton-coupled electron transfer

*Corresponding author: Naresh Kumar Katari, Department of Chemistry, School of Science, GITAM Deemed to be University, Hyderabad, India, e-mail: nkatari@gitam.edu
K Ganesh Kadiyala, Depatment of Chemistry, Shri Vishnu Engineering College for Women, Bhimavaram, Andhra Pradesh, India
Vanipenta Yamini, Sri A. S. N. M. Govt. College (A), Palakollu, Andhra Pradesh, India
Kommuru Goutham, Indian Institute of Chemical Technology, Hyderabad, Telangana, India

https://doi.org/10.1515/9783110788082-012

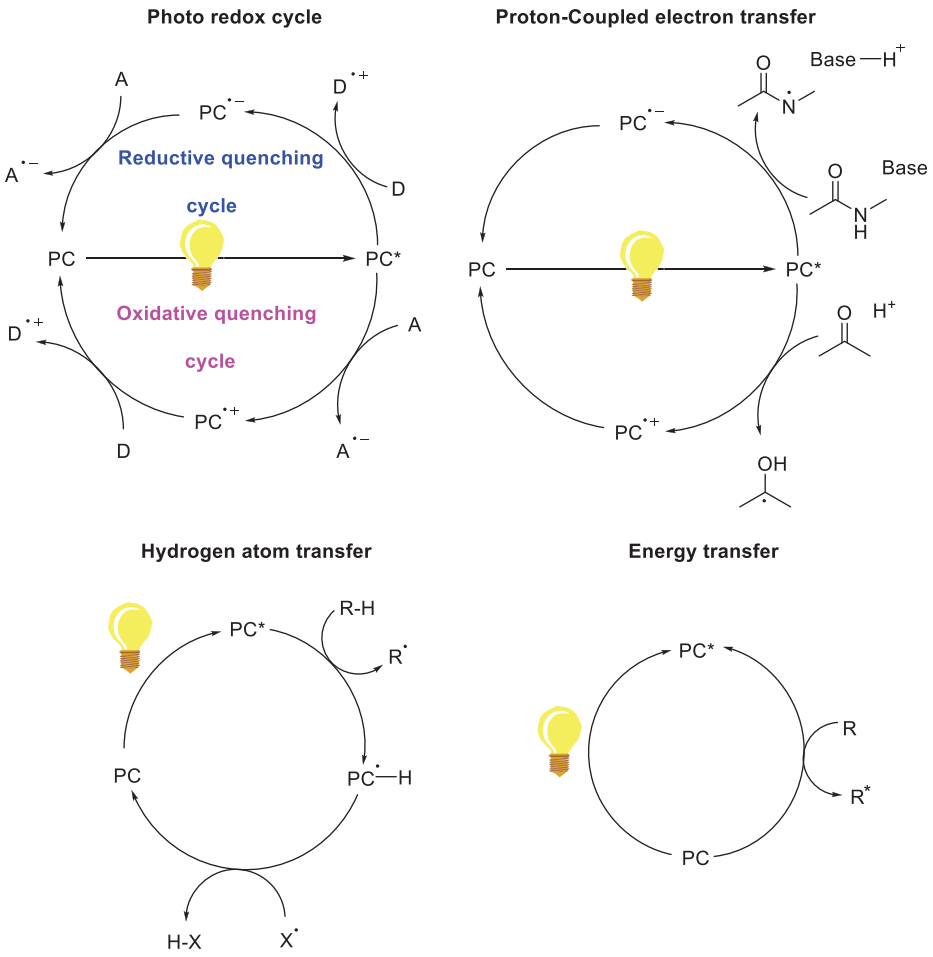

Figure 12.1: Distinct catalytic approaches of photocatalytic reactions.

[PCET]) could also work in tandem with the oxidative or reductive cycles. Contrarily, photocatalytic hydrogen atom transfer (HAT) occurs either following single electron transfer (SET) events or by the homolytic breakage of C–H bonds by the PC. Additionally, photocatalysts in their excited state can transfer their energy to reactants that are not capable of absorbing light to induce a chemical reaction.

12.3 Photosensitization

Zhang et al. [16] demonstrated the synthesis of Gd^{III} complexes that can serve as photosensitizer for singlet oxygen (Figure 12.2). These Gd^{III} complexes include porphyrin,

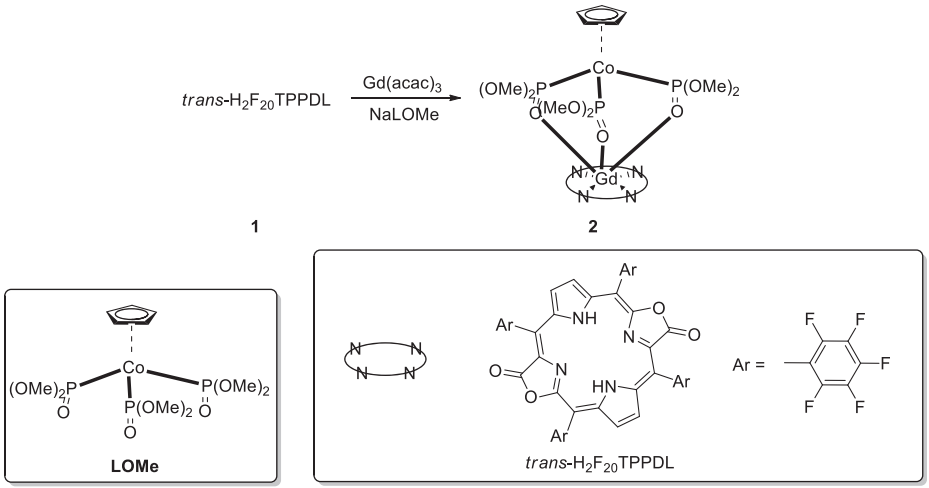

Figure 12.2: Synthesis of Gd^{III} *trans*-porphodilactone complex.

porpholactone, and *cis*- and *trans*-porphodilactone, which act as ligands that coordinate to Gd^{III} ion and alters its photosensitization efficiency. One of these ligands, *trans*-porphodilactone, produced singlet oxygen with high quantum yield when stimulated in the visible to near-infrared range (NIR). In addition to its photosensitization property, Gd(III) *trans*-porphodilactone complex (**2**) acts as effective catalyst for photooxidative C–H bond cleavage of secondary or tertiaryamines and also efficient in natural product cholesterol photo-oxygenation.

Schelter and coworkers [17] have developed luminescent Ce^{III} complexes with two complete mixed-ligand series (Figure 12.3). The general formula of Ce^{III} complexes is $[N(SiMe_3)_2]_{3-x}Ce^{III}[(Me_3Si)_2NC(N^iPr)_2]_x$ ($x = 0$, **3 N**; $x = 1$, **4 N**, $x = 2$, **5 N**; $x = 3$, **6 N**) and $(OAr)_{3-x}Ce^{III}[(Me_3Si)_2\ NC(N^iPr)_2]_x$ ($x = 0$, 1-OAr; $x = 1$, 2-OAr, $x = 2$, 3-OAr; $x = 3$, 4) has lifetimes of 117(1) ns and quantum yields of photoluminescence up to 0.81(2). These Ce^{III} photosensitizers are extensively studied for their photocatalytic activity in C–C bond formation between benzene and 4-fluoroiodobenzene.

12.4 Photoreductions

Ce^{III} complexes have been extensively studied by Schelter et al. [18] for the photoreduction reactions of benzyl chloride (**7**) through single electron transfer mechanism (SET) to furnish homo-coupled products (**9**) (Figure 12.4). The reaction involves the formation of $Ce^{IV}Cl$ complex which is a stronger absorber of light than Ce^{III} which leads to incomplete reaction. They anticipated that the addition of $NaN(SiMe_3)_2$ (**8**) might reduce $Ce^{IV}Cl$ complex to Ce^{III} with NaCl precipitation, preventing the formation of $Ce^{IV}Cl$ complex.

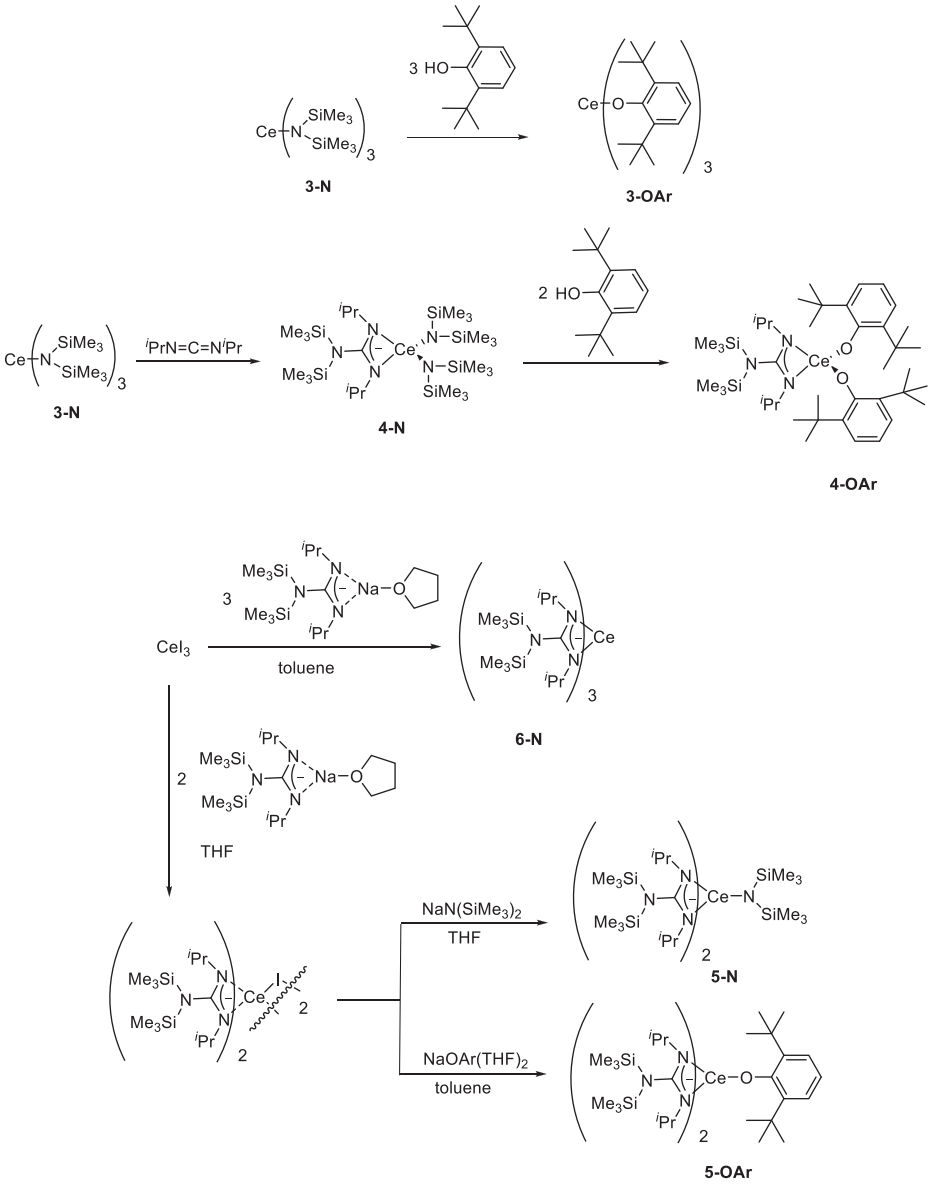

Figure 12.3: Synthesis of series of luminescent Ce^{III} complexes.

Pioneer in photocatalysis, Schelter and coworkers [19] revealed a robust method for the photo reduction of aryl chloride (**10**) to reduced aryl compounds (**11**) by using hexachlorocerate(III) $[Ce^{III}Cl_6]^{3-}$ (Figure 12.5). This complex is produced by in situ reaction of Et_4NCl and $CeCl_3$ in acetonitrile solutions (Figure 12.6). The main advantage

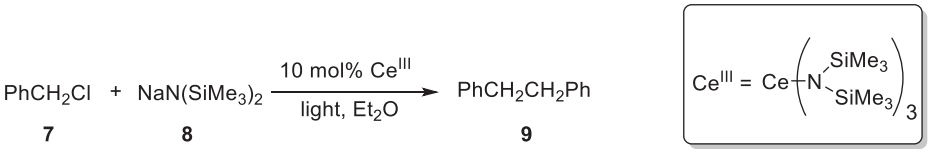

Figure 12.4: Photoreduction of benzyl chloride.

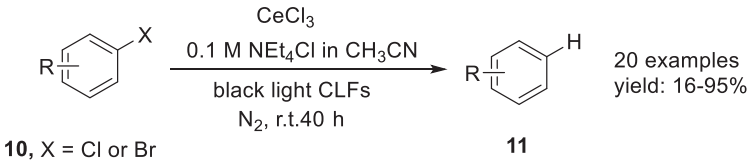

Figure 12.5: Photo reductive dehalogenation of aryl halides.

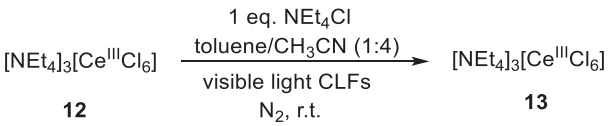

Figure 12.6: Synthesis of Ce^{III} complex.

of $[Ce^{III}Cl_6]^{3-}$ complex is the low photo reduction potentials and fast quenching kinetics which facilitates the dehalogenation of aryl chloride via aryl radical.

12.5 Photooxidations

Chen et al. [20] succeeded in developing an efficient protocol for the visible light driven photooxidation of diarylalkynes (**141**) to diketones (**15**) (Figure 12.7) and thioethers (**16**) to sulfoxides (**17**) (Figure 12.8). The team have prepared four isostructural lanthanides with same coordinated ligand 3,7-diamino-9,10-anthraquinone-2,6-disulfonatecomplexes via hydrothermal method. The complexes are $[Er(H_2O)_8]$•$[Er(\mathbf{L})(H_2O)_6]$•2 **L**•$8H_2O$ (**Er-L**), $[Tm(H_2O)_8]$• $[Tm(\mathbf{L})(H_2O)_6]$•2 **L**•$8.5H_2O$ (**Tm-L**), $[Yb(H_2O)_8]$•$[Yb(\mathbf{L})(H_2O)_6]$•2 **L**•$9H_2O$ (**Yb-L**), $[Lu(H_2O)_8]$ • $[Lu(\mathbf{L})(H_2O)_6]$•2 **L**•$9H_2O$ (**Lu-L**), respectively. Based on single crystal X-ray analysis, the structure of these complexes is determined, and it also discloses the presence of free and coordinated ligand in the crystal structure. These complexes act as heterogeneous photooxidative catalysts. Among the four lanthanide complexes, the **Er-L** is superior over other complexes for visible light driven photooxidation. The advantage of **Er**-photocatalyst includes easy isolation of catalyst after the completion of photooxidation through simple filtration, and it can be used without activation for up to five catalytic cycles.

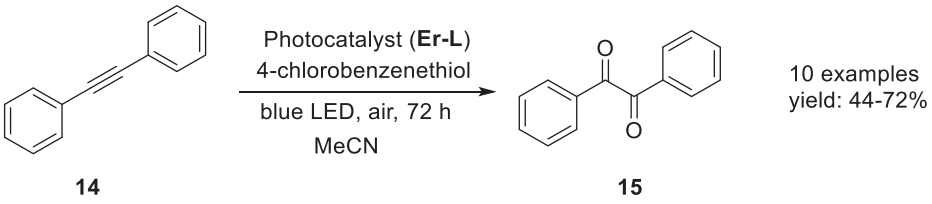

Figure 12.7: Photooxidation of arylalkynes to diketones.

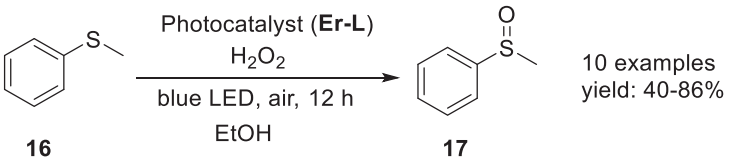

Figure 12.8: Photooxidation of thioethres to sulfoxides.

12.5.1 General procedure for the preparation of 3,7-diamino-9, 10-anthraquinone-2,6-disulfonic acid (H_2L)

2,6-Diamino-9,10-anthracenedione (4 g) was added gently to a stirring solution of 20 mL 20% oleum in 50 mL two-necked flask under cooling. To the reaction mixture H_2O_2 (30%, 0.5 mL) was added and run for 5 h at 100 °C. The resulting dark brown precipitate was filtered, washed cleanly with CH_3CN, and vacuum-dried to provide 5.4 g of product (a yield of 80%).

12.5.2 General procedure for the preparation $[Er(H_2O)_8]•[Er(L)(H_2O)_6]•2L•8H_2O$ (Er-L)

A mixture of H_2L (19.8 mg, 0.05 mmol) and $ErCl_3•6H_2O$ (38.2 mg, 0.1 mmol) was dissolved in a glass container into 3.0 mL water. The glass container was wrapped with a cap and heated to a temperature of 100 °C for 24 h. Then reaction mixture was gently cooled to room temperature to produce give reddish brown crystals, which were then filtered out, cleaned with CH_3COCH_3, and allowed to dry at ambient temperature. Yield: 65% according to H_2L.

12.6 Photocycloadditions

Anhua and coworkers [21] developed a robust [5 + 2] cycloaddition methodology upon reacting cycloalkonols (**18**) and electron deficient alkenes (**19**) by employing synergistic combination of a PET catalyst (photo-induced electron transfer catalyst–anthracene complex) and LMCT catalyst (cerium compound) for the construction of synthetically complex bridged lactones(**20**) (Figure 12.9). These bridged lactones are important scaffolds commonly found in natural products, such as hushinone [22], nepalactones [23], dendromonilisides [24], and tutin [25]. The process for the generation of alkoxy radical under SET mechanism is shown in Figure 12.10 by using photocatalyst anthracene complex. The reaction proceeds in a stepwise manner (Figure 12.11) in such a way that first the α-hydroxy C–C bond of alkoxy radical (**21**) could be selectively cleaved to give alkyl radical (**22**) and then undergo [5 + 2] cycloaddition with electron-deficient alkenes to give higher ring alcohol (**25**) followed by lactonization upon treatment with acid affording bridged lactones (**20**).

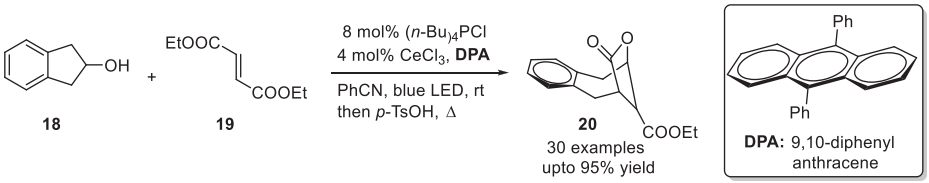

Figure 12.9: LMCT catalyst and PET catalyst-mediated photocycloaddition.

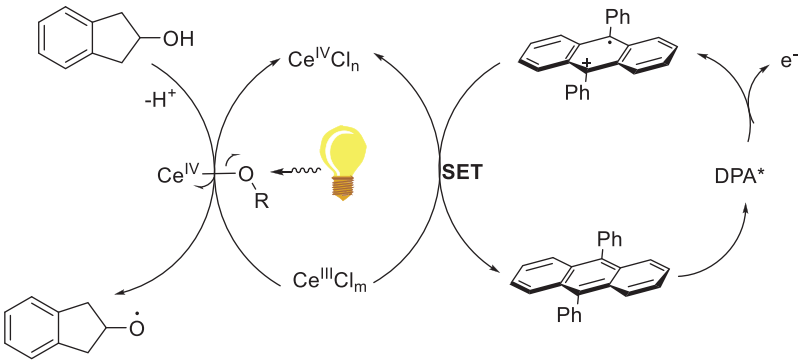

Figure 12.10: Generation of alkanol radical.

An efficient, mild and intermolecular [2 + 2] cycloaddition of indoles (**26**) with activated olefins (**27**) mediated by visible violet light-induced Gd(III) catalyst toward the construction of complex scaffolds cyclopenta[*b*]indoles (**28**) and indolines (**29**) (Figure 12.12) through one-pot, multistep fashion was developed by Glorious et al. [26]. The [2 + 2] cycloaddition takes place in an unusual head-to-head fashion rather than traditional head-to-tail

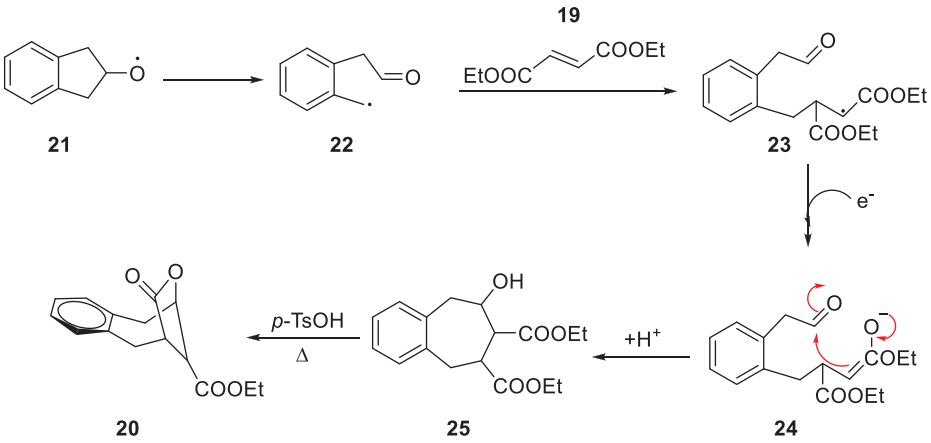

Figure 12.11: Photocycloaddition reaction mechanism.

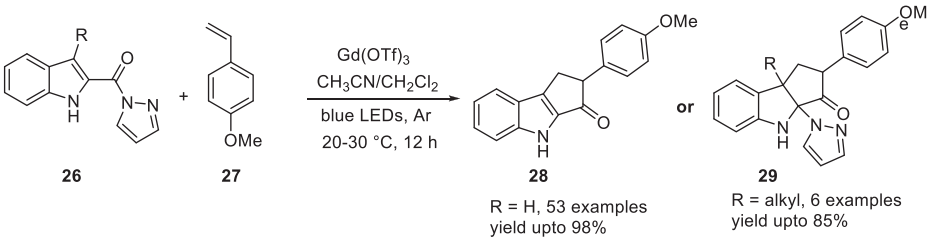

Figure 12.12: $Gd(OTf)_3$-induced photocycloaddition of indoles with alkenes.

fashion. The tethered pyrazole moiety acts as directing group when there is no substituent present at 3-position leads to cyclopenta[*b*]indole derivatives, whereas presence of substituent at 3-position, pyrazole moiety acts as both masking amination reagent and a directing group leads to dearomative cyclopenta[*b*]indoline derivatives (Figure 12.13).

12.7 Photocatalytic C–C/C–heteroatom bond construction

Zuo and coworkers [27] have developed an excellent and efficient straightforward protocol for C–C bond construction by employing inexpensive cerium photocatalysis (Figure 12.14). The reaction involves generation of in situ alkyl radical (**42**) upon irradiation of simple alcohols (**41**) by dehydroxymethylation (loss of formaldehyde). The obtained alkyl radical undergoes various cross-couplings, including hydrogenation, alkenylation, amination, alkylation, and oxidation under mild reaction parameters.

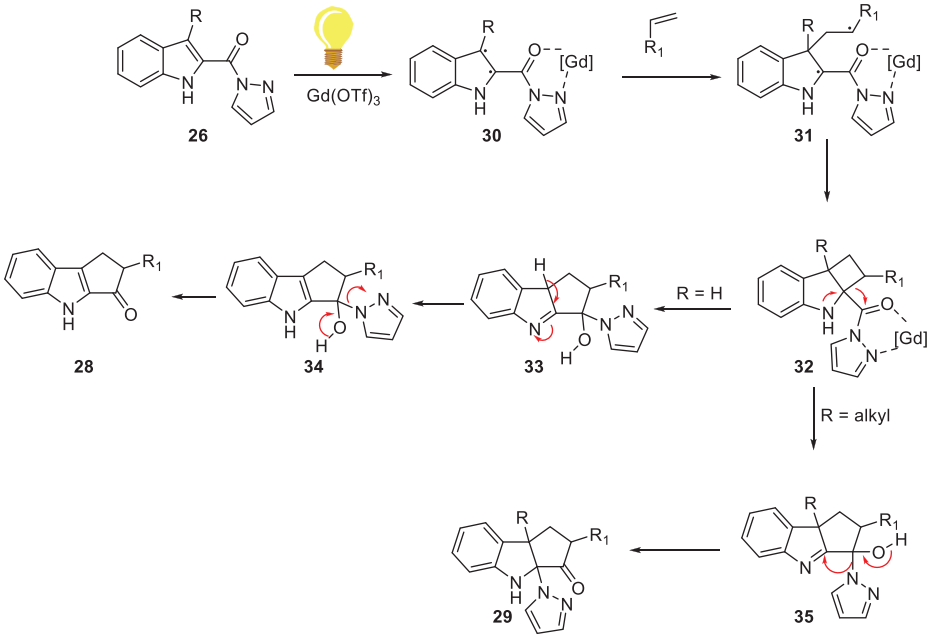

Figure 12.13: Mechanism of $Gd(OTf)_3$-induced photocycloaddition of indoles with alkenes.

Qiao et al. [28] achieved first-ever photo-induced Miyura borylation of sp^2 carbon by a rare earth photoreductant hexachlorocerate(III) anion $(Ce^{III}Cl_6)^{3-}$(Figure 12.15). The developed photo-induced Miyura borylation was coupled with Suzuki–Miyura reaction resulting in the preparation of variety of biaryls from aryl chlorides.

Zuo et al. [29] developed a general protocol for δ C–H activation of primary alcohols (**52**) by employing inexpensive cerium photocatalysis (Figure 12.16). The advantage of this method is that it does not require prefunctionalization of primary alcohols for distal functionalization. This protocol involves LMCT (ligand-to-metal charge transfer) mechanism (Figure 12.17) for the direct activation of substrates containing heteroatom functionalities.

Inspired by the previous work, Zuo et al. [30] realized the photo-induced rare earth metal catalyzed HAT (hydrogen atom transfer) strategy for the activation of highly inert substrates methane, ethane, propane, and butane (**58**) to form C-heteroatom bonds (Figure 12.18). The reaction sequence involves excitation of alcohol to form alkoxy radical which in turn triggers the inert alkanes to produce an alkyl radical which was then reacted with array of electron deficient substrates to form desired C–C/C–heteroatom bonds.

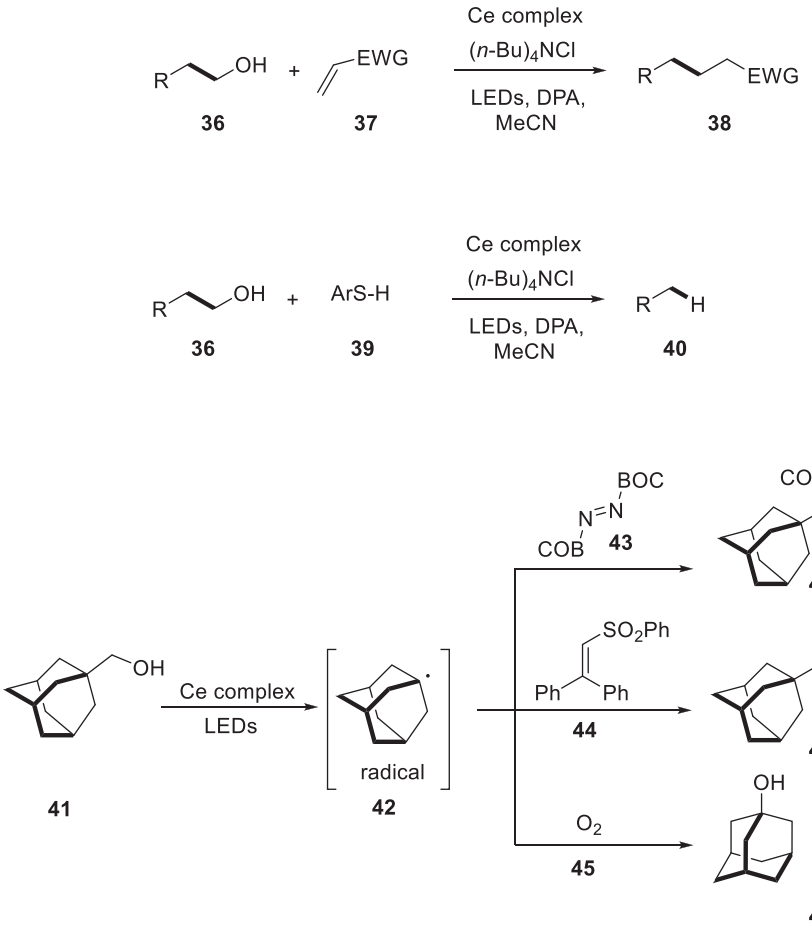

Figure 12.14: $CeCl_3$-induced photocatalytic C–H, C–C, and C–heteroatom bond-forming reaction.

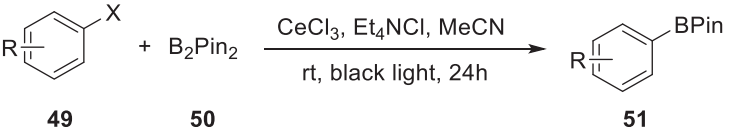

Figure 12.15: $CeCl_3$-induced photocatalytic C–B atom bond formation reaction.

12.8 Photocatalytic C–C bond cleavage

Guo and coworkers [31] demonstrated an efficient strategy for amination of cycloalkanols (**65**) by C–C bond cleavage through cerium complex catalyzed visible light-induced photoredox catalysis (Figure 12.19). This method is relevant to a wide array of

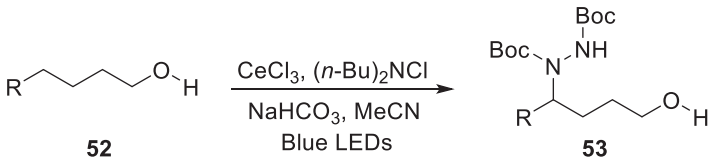

Figure 12.16: $CeCl_3$-induced photocatalytic δ C–H amination.

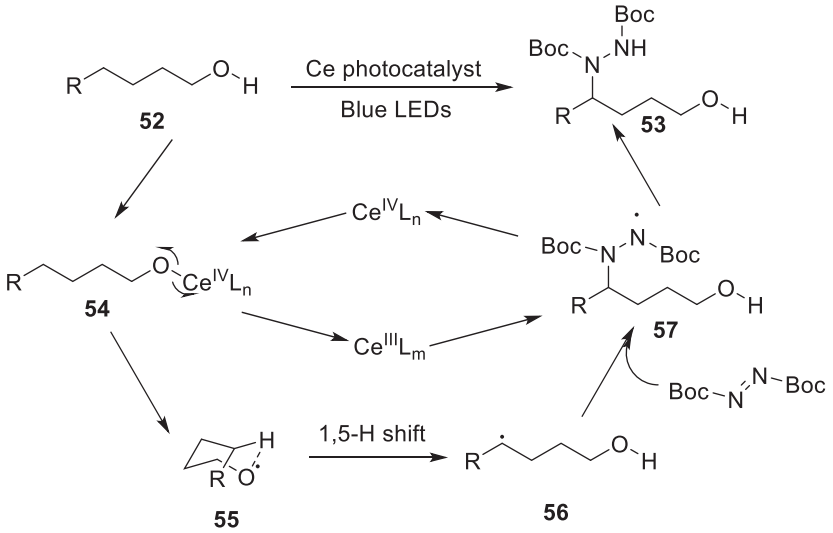

Figure 12.17: Mechanism of photocatalytic δ C–H amination.

secondary and tertiary cycloalkanols. The mechanism involves exposure of cerium chloride/alcohol complex (**67**) to radiation; the photo-excited state (**68**) is produced. The photo-excited Ce^{III} complex would result in a Ce^{IV} species (**69**) via a single electron transfer (SET) process with nitrogen radical intermediate (**71**). As anticipated, the extremely oxidized Ce^{IV} species (**69**) might facilitate the hard *β*-scission process to produce carbon radical (**70**). Then DBAD is coupled with extremely reactive radical species (**70**) to produce nitrogen-centered intermediate radical **71**, which subsequently produce the product through SET reduction (Figure 12.20).

Based on the previous C–C bond cleavage of cycloalkanols, the same group had continued the research on C–C bond scission of cyclic and acyclic ketones. They employed cooperative Lewis acid and cerium complex photocatalysis to selectively scission C–C bonds of different ketones by utilizing the ligand-to-metal charge transfer (LMCT) excitation method (Figure 12.21) [32]. This C–C bond scission reaction serves as an alternate to Norrish type l reaction. Many acyclic and cyclic ketones, ranging from straightforward, strained cyclobutanone (**72**) to intricate, less strained androsterone

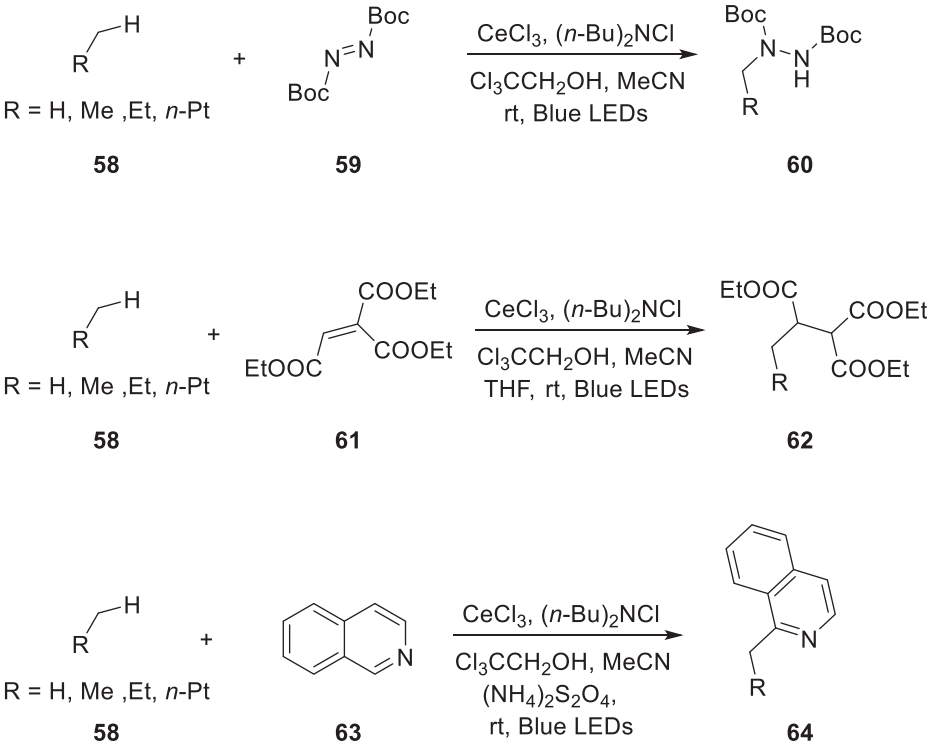

Figure 12.18: $CeCl_3$-induced photocatalytic inert sp^3 C–H amination, alkylation, and arylation.

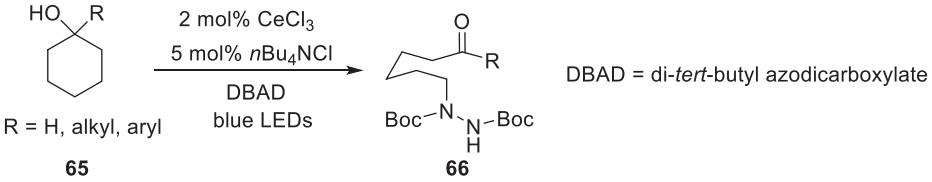

Figure 12.19: $CeCl_3$ Photo mediated C–C bond scission and amination.

(cyclopentanone) (**75**), could successfully undergo C–C bond scission and converted into useful chemical feed stocks. The obtained substrate from strained ketones was easily converted to desired lactams (**77**). The substrates from unstrained ketones (cyclohexanone), the C–C bond scission would result in the production of ω-aminated acyl cyanide (**76**), which would yield a carboxylic ester upon alcohol hydrolysis with a wide range of synthetic applications.

Coming over to linear ketone compounds (**77**), C–C bond scission was accomplished successfully, installing carboxylic ester (**78**) and hydrazine derivatives (**79**) at altered carbon fragments without any intervention of Norrish type II reaction (Figure 12.22). In

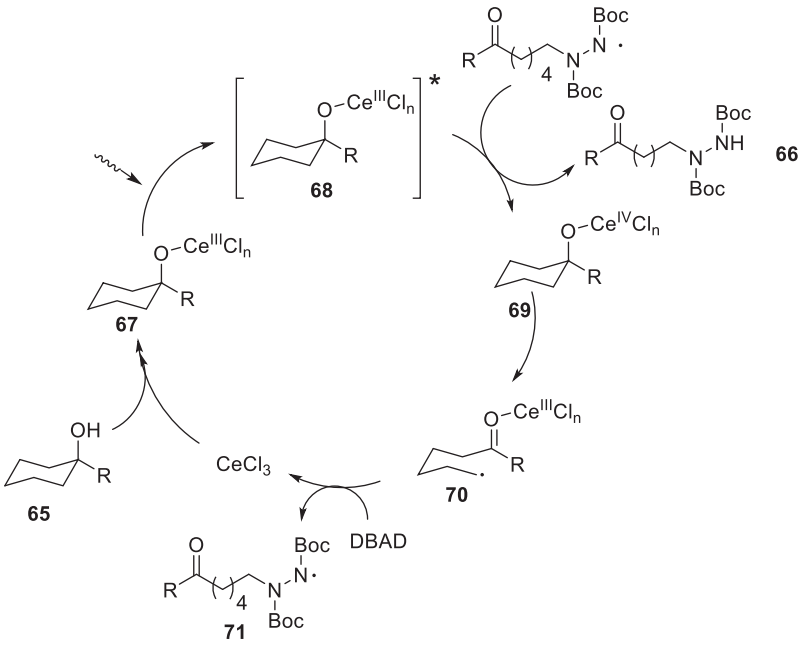

Figure 12.20: Proposed reaction mechanism of C–C bond scission and amination.

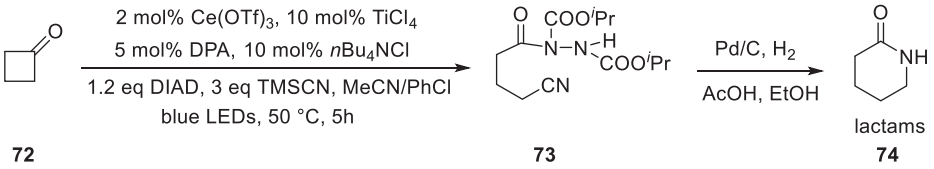

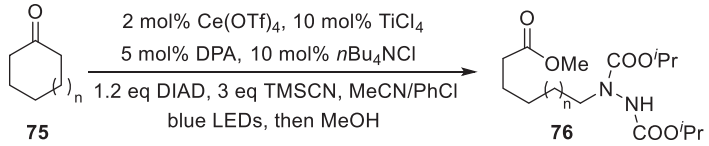

Figure 12.21: Cerium photocatalyzed C–C bond cleavage of strained ketones, unstrained.

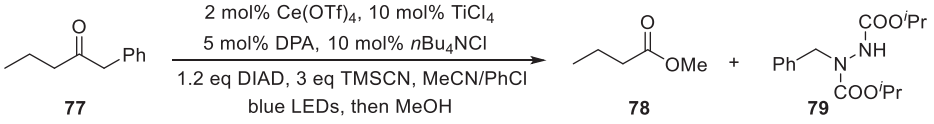

Figure 12.22: Cerium photocatalyzed C–C bond scission of acyclic ketones.

unsymmetrical linear ketones, more substituted α-C–C bond with greater stabilized radical could cleave precisely to furnish corresponding products.

Xiao et al. [33] published first report of cyanation of strained cyclopropylketones (**80**) via C–C cleavage by combining photoredox catalysis with Lewis acid catalysis (triple catalysis) and copper catalysis for the preparation of γ-cyanoketones (**82**) (Figure 12.23). The synthetic application of the present protocol has been showcased through the preparation of piperidine scaffolds (**84**) and (**85**) (Figure 12.24).

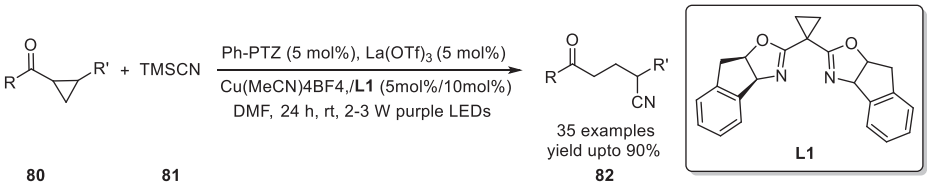

Figure 12.23: C–C bond scission of cyclopropylketones by triple catalysis.

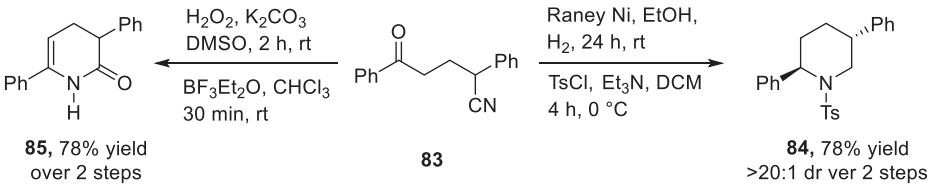

Figure 12.24: Synthetic utility of triple catalysis for the construction of piperidines.

12.9 Conclusions

In conclusion, rare earth metal complexes can act as redox-neutral Lewis acids as well as redox-active centers in photochemical reactions. The redox properties of rare earth complexes trigger the activation of halogen compounds, carboxylic acid derivatives, alcohols, unsaturated systems, and chalcogens, while switching to Lewis acid character they are able to activate a plethora of compounds containing carbonyl functionality. There is plethora of queries still unanswered with respect to mechanism of lanthanide photocatalysis.

References

[1] Skubi, KL, Blum, TR, Yoon, TP. Dual catalysis strategies in photochemical synthesis. Chem Rev, 2016, 116, 10035–10074.

[2] Shaw, MH, Twilton, J, MacMillan, DWC. Photoredox catalysis in organic chemistry. J Org Chem, 2016, 81, 6898–6926.

[3] Romero, NA, Nicewicz, DA. Organic photoredox catalysis. Chem Rev, 2016, 116, 1007–10166.

[4] Matsui, JK, Lang, SB, Heitz, DR, Molander, GA. Photoredox-mediated routes to radicals: The value of catalytic radical generation in synthetic methods development. ACS Catal, 2017, 7, 2563–2575.

[5] McAtee, RC, McClain, EJ, Stephenson, CRJ. Illuminating photoredox catalysis. Trends Chem, 2019, 1, 111–125.

[6] Tsui, E, Wang, H, Knowles, RR. Catalytic generation of alkoxy radicals from unfunctionalized alcohols. Chem Sci, 2020, 11, 11124–11141.

[7] Amos, SGE, Garreau, M, Buzzetti, L, Waser, J. Photocatalysis with organicdyes: Facile access to reactive intermediates for synthesis. Beilstein J Org Chem, 2020, 16, 1163–1187.

[8] Lee, Y, Kwon, MS. Emerging organic photoredox catalysts for organictransformations. Eur J Org Chem, 2020, 2020, 6028–6043.

[9] Bünzli, JC. Chapter 287-Lanthanide luminescence: From a mystery torationalization, understanding and applications. In: Handbook on the Physics and Chemistry of Rare Earths, 2016, vol 50, 141–176.

[10] Werts, MHV. Making sense of lanthanide luminescence. Sci Prog, 2005, 88(Pt 2), 101–131.

[11] Pitre, SP, Overman, LE. Strategic use of visible-light photoredox catalysis in natural product synthesis. Chem Rev, 2022, 122, 1717–1751.

[12] Marzo, L, Pagire, SK, Reiser, O, König, B. Visible-light photocatalysis: Does it make a difference in organic synthesis? Angew Chem Int Ed, 2018, 57, 10034–10072.

[13] Prier, CK, Rankic, DA, MacMillan, DWC. Visible light photoredox catalysis withtransition metal complexes: Applications in organic synthesis. Chem Rev, 2013, 113, 5322–5363.

[14] Narayanama, JMR, Stephenson, CRJ. Visible light photoredox catalysis: Applications in organic synthesis. Chem Soc Rev, 2011, 40, 102–113.

[15] Xuan, J, Xiao, WJ. Visible-light photoredox catalysis. Angew Chem Int Ed, 2012, 51, 6828–6838.

[16] Ke, XS, Ning, Y, Tang, J, Hu, JY, Yin, HY, Wang, GX, Yang, ZS, Jie, J, Liu, K, Meng, ZS, Zhang, Z, Su, S, Shu, C, Zhang, JL. Gadolinium(III) porpholactones as efficient and robust singlet oxygen photosensitizers. Chem Eur J, 2016, 22, 9676–9686.

[17] Yin, H, Carroll, PJ, Manor, BC, Anna, JM, Schelter, EJ. cerium photosensitizers: Structure–function relationships and applications in photocatalyticaryl coupling reactions. J Am Chem Soc, 2016, 138, 5984–5993.

[18] Yin, H, Carroll, PJ, Anna, JM, Schelter, EJ. Luminescent Ce(III) complexes as stoichiometric and catalytic photoreductants for halogen atom abstraction reactions. J Am Chem Soc, 2015, 137, 9234–9237.

[19] Yin, H, Jin, Y, Hertzog, JE, Mullane, KC, Carroll, PJ, Manor, BC, Anna, JM, Schelter, EJ. The hexachlorocerate(III) anion: A potent, benchtop stable, and readily available ultraviolet a photosensitizer for aryl chlorides. J Am ChemSoc, 2016, 138, 16266–16273.

[20] Zhu, TT, Tao, YT, Sun, Y, Wang, X, Zhang, XW, Chai, JL, Han, J, Zhao, XL, Chen, XD. Lanthanide complexes based on an anthraquinone derivative ligand and applications as photocatalysts for visible-light driving photooxidation reactions. JMolStruct, 2021, 1236, 130289–130293.

[21] Hu, A, Chen, Y, Guo, JJ, Yu, N, An, Q, Zuo, Z. Cerium-catalyzed formalcycloaddition of cycloalkanols with alkenes through dual photoexcitation. J Am Chem Soc, 2018, 140, 13580–13585.

[22] Klika, KD, Demirci, B, Salminen, JP, Ovcharenko, VV, Vuorela, S, CanBaşer, KH, Pihlaja, K. New sesquiterpenoid-type bicyclic compounds from the buds of betulapubescens − ring-contracted products of β-Caryophyllene?. Eur J Org Chem, 2004, 2004, 2627–2635.

[23] Wang, Y, Tian, J, Zhang, C, Luo, B, Gao, J. Picrotoxane sesquiterpene glycosides and a coumarin derivative from coriaria nepalensis and their neurotrophic activity. Molecules, 2016, 21, 1344–1352.
[24] Zhao, C, Liu, Q, Halaweish, F, Shao, B, Ye, Y, Zhao, W. Copacamphane, picrotoxane, and alloaromadendrane sesquiterpene glycosides and phenolic glycosides from Dendrobium moniliforme. J Nat Prod, 2003, 66, 1140–1143.
[25] Easterfield, TH, Aston, BC. XI. Tutu. Part I. Tutin and coriamyrtin. J Chem Soc Trans, 1901, 79, 120–126.
[26] Ma, J, Schäfers, F, Daniliuc, C, Bergander, K, Strassert, CA, Glorius, F. Gadolinium photocatalysis: Dearomative [2+2] Cycloaddition/Ring-Expansion sequence with indoles. Angew Chem Intd Ed, 2020, 59, 9639–9645.
[27] Zhang, K, Chang, L, An, Q, Wang, X, Zuo, Z. Dehydroxymethylation of alcohols enabled by cerium photocatalysis. J Am Chem Soc, 2019, 141, 10556–10564.
[28] Qiao, Y, Yang, Q, Schelter, EJ. Photoinduced miyaura borylation by a rare-earth-metal photoreductant: The hexachlorocerate(III) Anion. Angew Chem Intd Ed, 2018, 57, 10999–11003.
[29] Hu, A, Guo, JJ, Pan, H, Tang, H, Gao, Z, Zuo, Z. *δ*-Selective functionalization of alkanols enabled by visible-light-induced ligand-to-metal charge transfer. J Am Chem Soc, 2018, 140, 1612–1616.
[30] Hu, A, Guo, JJ, Pan, H, Zuo, Z. Selective functionalization of methane, ethane,and higher alkanes by cerium photocatalysis. Science, 2018, 361, 668–672.
[31] Guo, JJ, Hu, A, Chen, Y, Sun, J, Tang, H, Zuo, Z. Photocatalytic C-C bondcleavage and amination of cycloalkanols by Cerium(III) chloride complex. Angew Chem Intd Ed, 2016, 55, 15319–15322.
[32] Chen, Y, Du, J, Zuo, Z. Selective C-C bond scission of ketones via visible-lightmediated cerium catalysis. Chem, 2020, 6, 266–279.
[33] Liu, J, Liu, XP, Wu, H, Wei, Y, Lu, FD, Guo, KR, Cheng, Y, Xiao, WJ. Visible-light-induced triple catalysis for a ring-opening cyanationofcyclopropyl ketones. Chem Commun (Camb.), 2020, 56, 11508–11511.